FACTORS AFFECTING DROPLET SIZE DISTRIBUTIONS PRODUCED IN DISPERSED PHASE MIXERS

R. Mackelprang, J.A. Herbst, and J.D. Miller

Department of Metallurgy and Metallurgical Engineering
University of Utah
Salt Lake City, Utah 84112

ABSTRACT

Droplet size distributions were determined by stabilizing in gelatin and measurement of the distributions by means of computerized image analysis. Several variables that affect droplet sizes were studied and the resulting size distributions were modeled via a population balance equation. Key parameters in the model were related to the physical properties and operating conditions of the systems examined using a multiple linear approach.

FACTORS AFFECTING DROPLET SIZE DISTRIBUTIONS PRODUCED IN DISPERSED PHASE MIXERS

R. Mackelprang, J. A. Herbst and J. D. Miller

Department of Metallurgy and Metallurgical Engineering
University of Utah
Salt Lake City, Utah 84112

Introduction

Dispersed phase mixers are an important reactor type in several major industries and are becoming very popular in the metallurgical industry for the recovery of metal values from low grade aqueous solutions via solvent extraction. A key aspect of optimizing dispersed phase reactions, such as found in solvent extraction systems, is to understand the variables that affect the drop size distribution. The droplet size distribution and interfacial area are critical parameters of most solvent extraction systems since these often control the reaction rate between phases and may also influence significant economic issues such as organic losses, power consumption and capital-cost of equipment. Due to the wide use of mixer(s)/settler(s) in solvent extraction systems an important contribution can be made by quantifying the effect of important operating variables which determine the performance of these systems.

To accomplish this objective simple accurate measurements of the drop size distributions in the mixer must be made. Numerous techniques have been utilized for measuring drop size distributions including: chemical reactions (7); sedimentation techniques (1,9) simulation with hot wax (5,20) ; light transmission (3, 19, 24); dilution/stabilization techniques (17, 21); photographic techniques (4, 6, 8, 12, 14, 16, 20); and encapsulation techniques (14). Each technique has some advantages and limitations and each can be effective in certain systems or cases. Few, however can be used universally. Hence, after careful consideration of all of these techniques and after preliminary testing of many of these techniques, a dilution/stabilization technique known as gelatin embedding (17) was selected as the best possible method for stabilizing droplets in this project.

Finally, any complete description of a drop size distribution should include an accurate mathematical model for describing the size distribution. This model should also be useful for predicting size distributions in terms of the variables that affect it without introducing unnecessary complexity. In this regard a useful mathematical model was developed based on population balance concepts.

Experimental Systems and Techniques

The liquid-liquid system investigated in this project was studied at six different phase ratios and employed six organic and eight aqueous phases of different compositions. The standard organic phase was selected as a 10% by volume LIX 64N in 90% by volume Escaid 200, whereas the standard aqueous phase was selected as a 0.25 molar sodium sulfate solution which is believed to represent the ionic strength of typical industrial systems. A summary of the organic and aqueous phases used in this project is presented in Table 1. Details of these systems and their physical properties can be found elsewhere (13) (18).

The experimental equipment utilized in this project consisted of two agitating units, three different vessels and one impeller for mining. The primary agitation unit used was a Benco Model ELB Agitator which was mounted on a dynamo-meter stand and equipped with an Ametek Model L-2 force gage for power input measurements. This unit was capable of speed settings up to 1100 RPM and torque measurements of up to 20 in-lbs. A secondary agitating unit consisted of a Vickers hydraulic drive transmission assembly powered by a 5.0 horsepower motor. This unit was connected to the impeller shaft by a coupling arrangement which would also permit the insertion of a torque transducer for power measurements. High speeds and power inputs could be attained with this unit using small impellers.

The primary vessel used in this project was a modified, four liter beaker constructed of pyrex glass. This beaker was designed to allow for the mounting of four equally spaced baffles of 1.3 cm and provided with an enlarged spout to facilitate sampling. This vessel had an inside diameter of 15.9 cm and was run at a constant volume of 3.25 liters or a liquid depth of 17.2 cm in a batch mode. A similar vessel to this was utilized for the continuous tests and a somewhat different, totally enclosed vessel of larger volume was used for the high speed tests, details of these are reported eleswhere (13).

The only impeller employed in this project was a single, flat blade turbine impeller with a diameter of 6.35 cm and a blade height of 0.8 cm. The impeller was constructed of 316 stainless steel and came with the ELB agitator kit.

The sampling procedure was essentially the same regardless of the agitating equipment or vessel being used. The organic droplets inside the vessel were sampled by withdrawing a small amount of emulsion from the desired point in the vessel by means a small siphon. These small siphons were constructed from 3 mm diameter glass tubing by heating and bending into a "V" shape. Generally this construction allowed the

Table 1. Aqueous and Organic Phase Composition and Physical Properties

System	Composition	pH	Ionic Strength	Density (g/cc)	Viscosity (poise x 10^2)
Aqueous 1	Distilled Water	6.4	0.000	1.00	1.00
Aqueous 2	.25 M Na_2SO_4	6.8	0.750	1.03	1.18
Aqueous 3	.875 M Na_2SO_4	7.2	2.625	1.10	1.61
Aqueous 4	1.50 M Na_2SO_4	7.7	4.500	1.17	2.16
Aqueous 5	.25 M Na_2SO_4 + .0826 M H_2SO_4	2.0	1.000	1.03	1.26
Aqueous 6	.25 M Na_2SO_4 + .1815 M NH_4OH	11.0	0.930	1.03	1.26
Aqueous 7	.25 M Na_2SO_4 + .0826 M H_2SO_4 + .051 M $CuSO_4$	2.0	1.100	1.03	1.26
Aqueous 8	.225 M $NaHCO_3$ + 0.225 M Na_2CO_3	9.8	1.35	1.04	1.30
Organic 1	Escaid 200			0.751	1.49
Organic 2	Cyclohexane			0.761	0.762
Organic 3	Xylene			0.860	0.610
Organic 4	Isooctane			0.693	0.520
Organic 5	10% LIX in 90% Escaid 200			0.764	1.720
Organic 6	5% Adogen 383 in 95% Xylene at 0.076 M Sebacyol Chloride			0.900	0.650

siphon to be placed in the sample lip of the vessel in a manner such that the outside stem of the siphon was vertical while the inside stem was located at the desired sampling point which was usually at a point mid-way between the liquid surface and the impeller and mid-way between the vessel wall and the impeller shaft.

Once in place, the siphon was initiated and allowed to run briefly after which a couple of drops of emulsion were allowed to fall into a petri dish containing 4 to 6 ml of freshly prepared, 8% by weight pigskin gelatin solution at 28° to 30°C. The emulsion drops were mixed briefly and the gelatin solution manipulated to allow the formation of a thin layer of gelatin with representative drops to cover the bottom of the petri dish. The petri dish was then immediately placed in an ice water bath where it solidified almost instantly after which it was scanned microscopically for quality. Poor quality samples were discarded whereas good samples were refrigerated at 10°C and then analyzed within the next 24 hour period.

Most samples were analyzed using the Quanta Met 720, a computerized image analyzer that counts and sizes the embedded drops. A minimum of 300 drops per sample were sized in this manner, however, as many as 1000 per sample were often counted.

Experimental Results

The major variables affecting drop sizes which were investigated in this project include: (1) the time to reach equilibrium; (2) speed/power input; (3) phase ratio or phase fraction; (4) the presence and absence of an extractant-LIX74N, (5) the behavior of pure diluents; (6) the rate of mass transfer across the interface; (7) aqueous phase pH; and (8) aqueous phase ionic strength. The ability to predict continuous flow distributions at steady state from batch data was also examined.

The approach to equilibrium or steady state was investigated mainly to note the appropriate time for sampling to obtain a true steady state sample. The approach to equilibrium was noted to be a complex function of several variables of which speed/power input and phase fraction are the most significant. Therefore, a high phase fraction system agitating at a low speed was chosen as a limiting case with all subsequent cases to be tested utilizing higher speeds and lower phase fractions and hence shorter times for equilibrium to occur. The test consisted of taking samples at times of; 1.25, 2.5, 5.0, 10.0 20.0, 30.0, 40.0, and 50 minutes after the start of agitation. It was found upon analysis of these respective size distributions that significant changes occurred for times up to 30.0 minutes. Thus all subsequent tests were conducted after allowing a miniumum of thirty minutes for equilibrium to occur.

The experimental design performed on the standard system consisted of four levels of phase ratio; 0.2, 0.3, 0.4, and 0.5 and three levels of speed/power input; 450rpm/2.5×10^{-3} HP, 550rpm/3.7×10^{-3} HP, and 650rpm/5.7×10^{-3} HP. Typical results are illustrated in Figure 1 for speed/power inputs at two levels of phase fraction and Figure 2 where four levels of phase fraction are illustrated at two levels of speed. The results of these tests concur with the general

findings of other researchers, i.e., an increasing fineness of droplet size distribution as the speed/power input increases and as the phase fraction decreases.

The effect of mass transfer on the droplet size distribution was studied by adding copper as dissolved cupric sulfate to the standard system at a pH of 2.0 and then sampling the size distribution at times of: 0, 20, 40, 80, 160, 320 and 1800 seconds after addition.

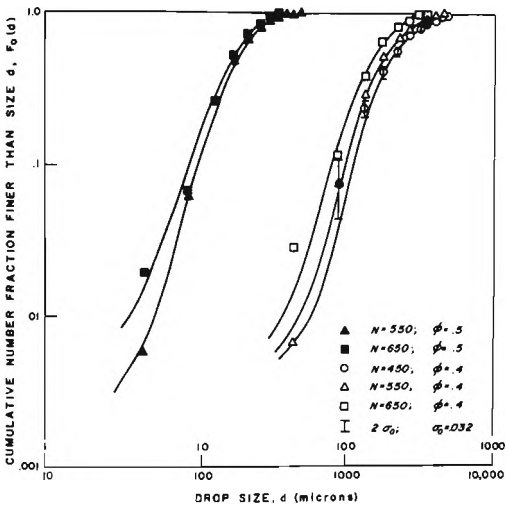

FIGURE 1. The effect of speed/power input at phase fractions of .5 and .4 in the standard system (Upper scale right side plots, lower scale left side plots).

The respective size distributions for these times were noted to differ very little and hence it is concluded that mass transfer in this system has no effect on droplet size distribution which is not too surprising since the physical properties of the system remained relatively constant.

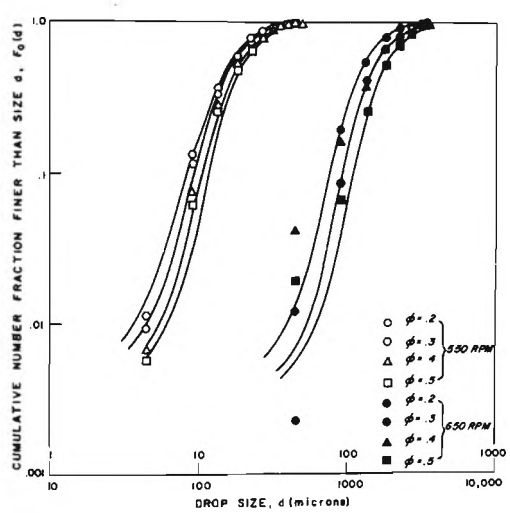

FIGURE 2. The effect of phase fraction at speeds of 550 and 650 rpm in the standard system (Upper scale right side plots, lower scale left side plots).

The effect of the presence of the extractant, LIX 64N, as 10% of the organic volume was evaluated by comparing the size distribution obtained in a pure Escaid 200 system to the size distribution of a system in which the organic phase contained 10% LIX 64N. The results are given in Figure 3 which shows the size distributions for the pure Escaid 200 system to be significantly coarser than the 10% LIX 64N system.

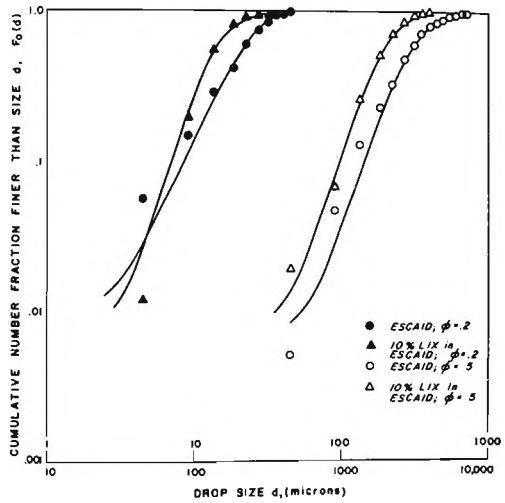

FIGURE 3. The effect of LIX 64N presence in Escaid 200 on the drop size distribution at a speed of 650 rpm in the standard aqueous system (Upper scale right side plots, lower scale left side plots).

This phenomenon can be explained in terms of the effect of the LIX 64N concentration on the liquid/liquid interfacial tension. With LIX 64N present, the interfacial tension was found to be 16.2 dynes/cm as compared to 45.2 dynes/cm for the pure Escaid. The lower interfacial tension results in a lower resistance to breakage forces, hence a finer drop size results. Essentially the same behavior was noted when other diluents with similar interfacial tensions such as isooctane and cyclohexane were used. Pure xylene with a lower interfacial tension than any of the other diluents again displayed a finer size distribution.

The variation in droplet sizes caused by changes in the aqueous phase composition was also investigated. Obviously the most common changes in the aqueous phase are those resulting from dissolved salts or ionic strength and changes in pH.

The effect of dissolved salts or ionic strength level was studied by measuring the change in the size distribution at four levels of sodium sulfate addition. The results are illustrated in Figure 4 and indicated that small additions of salt have little effect on the droplet size distribution while large addition of salt causes the distribution to become progressively finer. The explanation for this phenomenon arises from changes in the physical properties of the aqueous phase, namely density and viscosity which are changing to promote breakage, and also as a result of electrostatic surface forces. In the latter case preferential adsorption of an ion at the organic surface may lead to droplet charging or the formation of a dense double layer which inhibits coalescence and

enhances droplet shattering during breakage.

The pH of the aqueous phase in the standard system

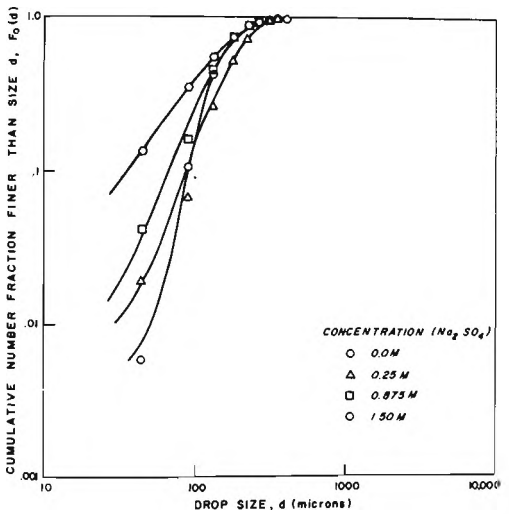

FIGURE 4. The effect of aqueous ionic strength on size distribution in the LIX 64N/Escaid 200 system at a phase fraction of .5 and speed of 650 rpm.

was also noted to affect droplet size distribution appreciably in some cases. Here it was found that size distributions from low and high pH ranges differed from those at moderate pH ranges. The change was most dramatic in the case of high pH's as shown in Figure 5.

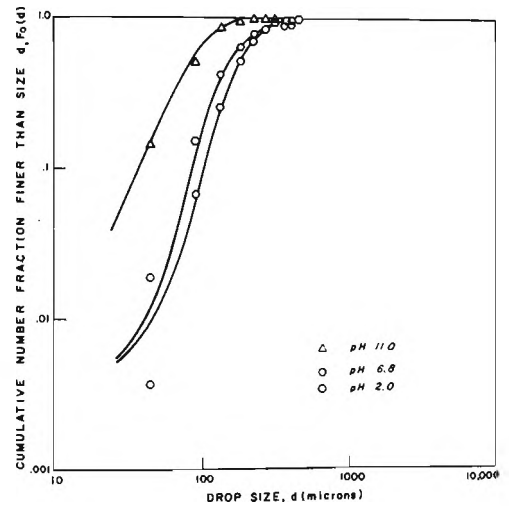

FIGURE 5. The effect of aqueous pH on drop size distribution in the standard organic system at a phase fraction of .5 and a speed of 650 rpm.

The size distribution at a pH of 11 was much finer than at lower pH's. This behavior was again traced to a large decrease in interfacial tension which changes from 16.2 dynes/cm at moderate pH to about 5.2 dynes/cm, at a high pH - a decrease of over two thirds. These results may reflect the conversion of the acid form of the extractant into the sodium salt which could significantly alter the interfacial tension and electrostatic forces thus accounting for the fine drop size distribution.

The less drastic changes in size distributions that occur at low pH are not conclusive and should be checked at very low pH values which may display variations more clearly. Nevertheless, it is thought that lowering the pH may affect the charge on the drops and hence droplet electro-kinetic behavior which in turn may influence breakage and coalescence mechanisms.

The last topic of interest investigated in this project was the appropriateness of using batch tests to simulate continuous tests in the LIX 64N/Escaid 200 -acid/sulfate system. These tests were performed in a slightly different vessel which was modified for continuous flow. The size distributions produced by this vessel in the batch mode were compared to the size distributions generated in the continuous mode with retention times of 2.16 and 0.54 minutes. The results are shown in Figure 6 and indicate that very similar size distributions occur between batch tests and continuous tests with moderate to high retention times.

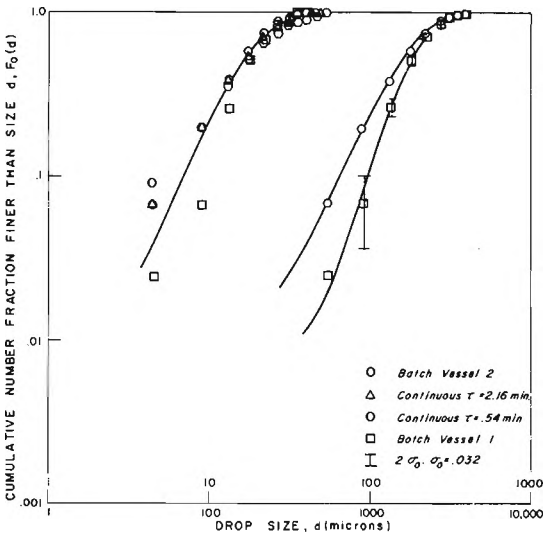

FIGURE 6. Drop size distribution differences produced by vessels one and two and continuous mode operations with the standard system at a phase fraction of .5 and a speed of 650 rpm (Upper scale right side plots, lower scale left side plots).

At short retention times the agreement becomes worse and thus the simulation is worse. However, we can conclude from these results that batch tests can be used to simulate continuous tests run at moderate to high retention times.

Mathematical Model

Mathematical models for describing drop size distributions are numerous and varied. Several models have utilized a population balance approach with good success (2, 5, 23), but have incorporated some questionable assumptions, manipulations and excessive complexity into their development and use. Hence it was desired to examine these models in an effort to

improve on their utility.

Since the scope of this topic is rather extensive it is impossible to report all the details of the model development here. Instead a general outline will be presented. The details of the model development are given elsewhere (13, 25).

The model development begins with the macroscopic population balance equation initially proposed by Hulbert and Katz (10):

$$\frac{1}{V}\frac{\partial}{\partial t}\{V\bar{\psi}(\underline{\zeta},t)\} = -\sum_{j=1}^{J}\frac{\partial}{\partial \zeta_j}\{\dot{x}_j\bar{\psi}(\underline{\zeta},t)\} - \bar{D}(\underline{\zeta},t) + \bar{B}(\underline{\zeta},t) + \frac{1}{V}(Q_{in}\bar{\psi}_{in} - Q_{out}\bar{\psi}_{out}) \quad (1)$$

The term on the left hand side of Equation 1 represents the overall time rate of change in the average population density function for a droplet assembly. Where $\bar{\psi}(\underline{\zeta},t)d\underline{\zeta}$ gives the number of particles in a system per unit volume ($\underline{\zeta}$ represents the transposed vector of properties $\zeta_1, \zeta_2, \zeta_3 \ldots \zeta_n$). The first term on the right hand side represents the change in properties resulting from continuous processes such as mass transfer while the next two terms represent the changes occuring as a result of catastrophic processes such as breakage and coalescence events. The final term on the right hand side represents changes due to flow in and out of a vessel.

We now proceeed to make the following initial assumptions and simplifications for the mixer:

(1) The system being modeled is a batch mixer and hence flow in and out are zero ($Q_{in} = Q_{out} = 0$)

(2) The volume in the mixer is constant, hence the volume terms, V, cancel from each term in the equation

(3) The model is concerned with only one property ζ_1, that being droplet size expressed as volume v, and a size distribution represented as a number density functon by volume, $\psi(v,t)$.

(4) Size changes due to continuous processes such as chemical reactions are negligible, thus $\dot{x}_1 = d\zeta_1/dt$ is eliminated from the equation.

(5) The system being modeled is isothermal and homogeneous and will approach a state of equilibrium in a finite time. Equation (1) therefore reduces to:

$$\partial/\partial t\{\bar{\psi}(v,t)\} = \bar{B}(v,t) - \bar{D}(v,t) = \bar{B}_b(v,t) + \bar{B}_c(v,t) - \bar{D}_b(v,t) - \bar{D}_c(v,t) \quad (2)$$

Where the subscripts b, c, refer to the processes of breakage and coalescence respectively, hence $\bar{B}_b$ refers to the birth of drops due to breakage and so forth.

Each term on the right hand side of Equation 2 must now be developed individually and thus we begin with the term $\bar{D}_b(v,t)$ since it is the most basic to the model development. We are interested here in obtaining an expression for the death of droplets due to breakage of drops in any given interval v to v+dv per unit time and volume which we shall represent as:

$$\bar{D}_b(v,t)dv = -S(v,t)\bar{\psi}(v,t)dv \quad (3)$$

Here the term S(v,t) is known as the selection function which is a lumped parameter representing the fraction of droplets of a given size which are breaking per unit time. For simplicity it is assumed that the selection function is independent of time and is proportional to droplet "size" as represented in Equation 4;

$$\bar{D}_b(v,t)dv = -kv^m\bar{\psi}(v,t)dv \quad (4)$$

where k is a constant. The exponent m will take on a value of unity for breakage rates proportional to drop volume, two thirds for rates proportional to drop area, one third for rates proportional to drop diameter and zero if the breakage rate is independent of drop size.

Likewise the term representing the birth due to breakage of new drops into the interval v to v+dv from all larger intervals v to v_{max} can be represented as:

$$\bar{B}_b(v,t)dv = \int_v^{v_{max}} b(v,v')\,kv'^m\bar{\psi}(v',t)dv'dv \quad (5)$$

Where b(v,v') is known as the breakage function and represents the number of daughter droplets of size v resulting from a breakage of a droplet of size v'. An assumption now must be made as to the form of b(v,v'). In this case it was assumed that binary breakage occurs producing a uniform distribution of daughter drops. Equation 5 then becomes:

$$\bar{B}_b(v,t)dv = \int_v^{v_{max}} 2kv'^{(m-1)}\bar{\psi}(v',t)dv'dv \quad (6)$$

Now turning to the contributions of coalesence events we can state that the death of droplets out of this interval via coalescence events over the range of all interval sizes, v_{min} to v_{max}-v is represented as:

$$\bar{D}_c(v,t)dv = -\int_{v_{min}}^{v-v_{max}}\lambda(v,v',t)\,\bar{\psi}(v,t)\,\frac{\bar{\psi}(v',t)}{\bar{n}(t)}\,dv'dv \quad (7)$$

Where the term $\lambda(v,v',t)$ is known as the coalescence function which represents the probability that a drop of size v will coalesce with a drop of size v' in a dt of time. The form of this function has been assumed to be constant, hence independent of droplet size and time. Furthermore, if V_{max} is assumed to be large with respect to dv', the integration of Equation 7 gives:

$$\bar{D}_c(v,t)dv = -\lambda\bar{\psi}(v,t)dv \quad (8)$$

Finally the birth of droplets into the interval v to v+dv from coalescence events occuring among drops from all smaller size intervals from v_{min} to the size v can be represented as:

$$\overline{B}_c(v,t)dv = \frac{\lambda}{2}\frac{1}{\overline{n}(t)}\int_{v_{min}}^{v}\overline{\psi}(v-v',t)\overline{\psi}(v',t)dv'dv \qquad (9)$$

Combining each of these respective expression into the reduce population balance equation and rearranging gives:

$$\frac{\partial}{\partial t}\left(\overline{\psi}(v,t)\right) = -\overline{\psi}(v,t)\{kv^m+\lambda\} + 2k\int_{v}^{v_{max}} v'^{(m-1)}\overline{\psi}(v',t)dv'$$

$$+ \lambda/2\overline{n}(t)\int_{v_{min}}^{v}\overline{\psi}(v-v',t)\overline{\psi}(v',t)dv' \qquad (10)$$

The form of this equation now requires that the parameters k, λ, m and v_{max} be specified prior to obtaining a solution. However, by making the equation dimensionless we can eliminate the parameters k, λ and thereby attempt solutions by choosing various values for the parameter m (from zero to one) once a reliable estimate of v_{max} is obtained.

The following non dimensional quantities are proposed for making Equation 10 dimensionless:

$$v_o = (\lambda/2k)^{1/m} \qquad (11)$$

$$t_o = 1/\lambda \qquad (12)$$

$$v^* = v/v_o \text{ and } dv^* = dv/v_o \qquad (13)$$

$$t^* = t/t_o \text{ and } dt^* = dt/t_o \qquad (14)$$

$$f_o(v,t) = f_o^*(v^*,t^*)/v_o \qquad (15)$$

$$\overline{n}^*(t^*) = \overline{n}(t)/\overline{n}(0) \qquad (16)$$

$$\overline{\psi}^*(v^*,t^*)dv^* = \overline{n}^*(t)f_o^*(v^*,t^*)dv^* \qquad (17)$$

Upon substituting these expressions into Equation 10 one obtains:

$$\partial/\partial t^*\left\{\overline{\psi}^*(v^*,t^*)\right\} = -\overline{\psi}^*(v^*,t^*)\left(1+\frac{v^{*m}}{2}\right)$$

$$+ \int_{v^*}^{v^*_{max}} v'^{*\,m-1}\,\overline{\psi}^*(v'^*,t^*)dv'^* \qquad (18)$$

$$+ 1/2\overline{n}^*(t^*)/\overline{n}(0)\int_0^{v^*}\overline{\psi}^*(v^*-v'^*,t^*)\overline{\psi}^*(v'^*,t^*)dv'^*$$

The solutions for the selected values of the parameter m were generally obtained by using a fourth order interpolating polynomial to integrate and a fourth order Adams-Bashforth-Moulton method to differentiate (13). However, it was found that for the case of m=1 an analytical solution was possible (25) in the steady state form of Equation 18 which produces an exponential number density function, $f_o(v)$, with a dimensionless mean size of 1.0, that is:

$$f_o(v) = \frac{1}{v_o}e^{-v/v_o} \qquad (19)$$

Numerical solutions for the cases where the parameter m equals 1, 2/3, 1/3 and 1/6, corresponding to selection functions which are proportional to drop volume, drop area, drop diameter and the square root of the drop diameter, are shown in Figure 7.

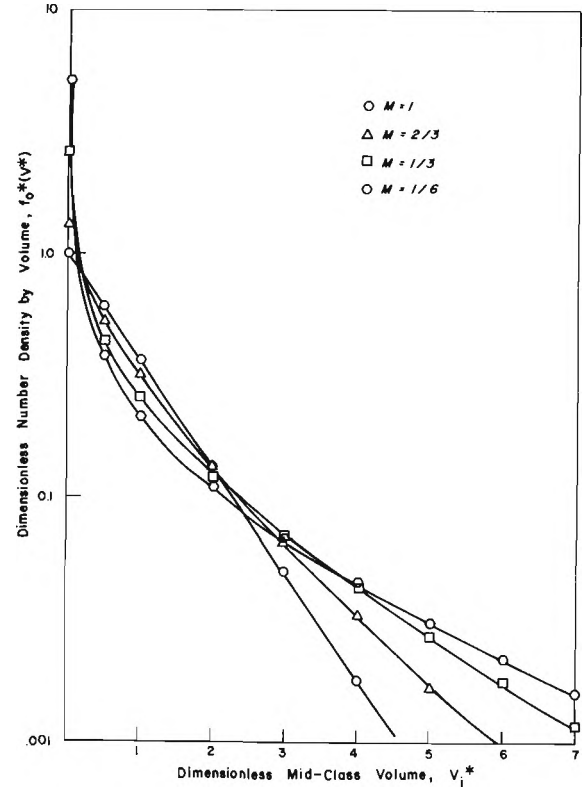

FIGURE 7. Dimensionless drop size distributions generated by the population balance Equation 18 for a batch mixer.

The formulation of the dimensionless population balance equation results in the recognition of the importance of the parameters m and v_o. Therefore, to fully utilize and develop the potential of the model it becomes necessary to relate these parameters to the system properties and operating conditions.

The parameter m is the single most important parameter of the model since it stresses the importance of breakage processes on the droplets as well as the final form of the mathematical solution and, in this regard, can be thought of as a distribution modulus.

The solutions to the model for various cases of m indicates that larger values of m result in coarser size distributions than those with smaller values of m. This behavior suggests that the parameter m can be related to system variables and operating conditions. To test this possibility an empirical equation developed from knowledge of important liquid physicochemical properties and operating conditions was constructed. Important variables were grouped together in dimensionless groups via Buckingham Pi Theory and the coefficients and exponents determined by multiple linear regression on experimental data. Values for the parameter m were selected by plotting each set of experimental data transformed to dimensionless form against the dimensionless distributions generated by

the model for several cases of the parameter m and then choosing the value of m that best explained the experimental data. Hypothesis tests were then performed on each term to test its significance in the model. The final accepted equation for m was:

$$m = e^{0.19}\,(1+\phi)^{1.76}\,(\nu_d/\nu_c)^{0.37}\,(H/D)^{0.52}\,(N'_{we})^{-0.38} \qquad (20)$$

The parameter v_o on the other hand is the basis for converting to or from the dimensionless form and is the basis for the simplified model. The parameter v_o is also a function of the other parameters k, λ, and m and has the units of volume and hence may be thought of as a characteristic size or volume. The parameter v_o is readily obtained from the dimensionless mean size or volume, which is determined both from the numerical solution to the population balance equation for each value of m, and from the dimensional mean size of the experimental data by the relation:

$$v_o = \bar{v}/\bar{v}^* \qquad (21)$$

The dependence of the dimensionless mean size, which is a function of v_o, on the parameter m is shown in Figure 8 and is seen to be approximately linear.

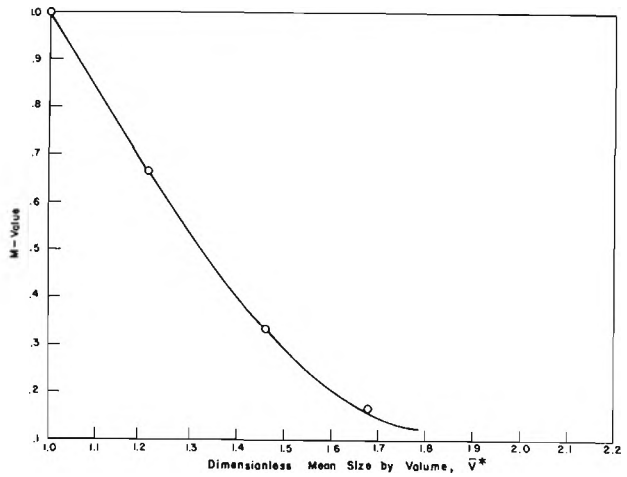

FIGURE 8. The parameter m as a function of the dimensionless mean size by volume.

It may be obvious by now that once the parameter m can be predicted as by Equation 20 and the corresponding dimensionless mean size estimated from Figure 8 all that remains is to predict the dimensional mean volume. At this point all the major parameters of the model are known and the size distribution can be determined.

Since the mean size can be related to the parameter v_o which in turn is a function of the parameter m; it seems logical to assume that the mean size is a function of the same variables that determine the parameter m. (Independent considerations of the factors affecting the mean size will lead to the same conclusion.) Hence developing an analogous expression for the mean size by the same method as that used to develop the expression for the parameter m we get:

$$\bar{V} = D^3\, e^{-6.37}(H/D)^{-1.24}(\bar{I})^{0.03}(N'_{we})^{-1.54}(\phi)^{0.89} \qquad (22)$$

The large dependence of this equation on the impeller size, D, is the result of the dimensionless analysis by the Buckingham Pi Theory and unfortunately limits this equation to systems with similar sized impellers to the one used here.

Dimensionless Correlation of Experimental Data and Prediction of Dimensional Size Distributions

The experimental data generated in this project was transformed into dimensionless form utilizing m-values calculated from Equation 20 and v_o values calculated from the data mean sizes with assistance from Figure 8. Examples of experimental data that fit the model predictions for various cases of the parameter m are shown in Figures 9, 10, 11 and 12.

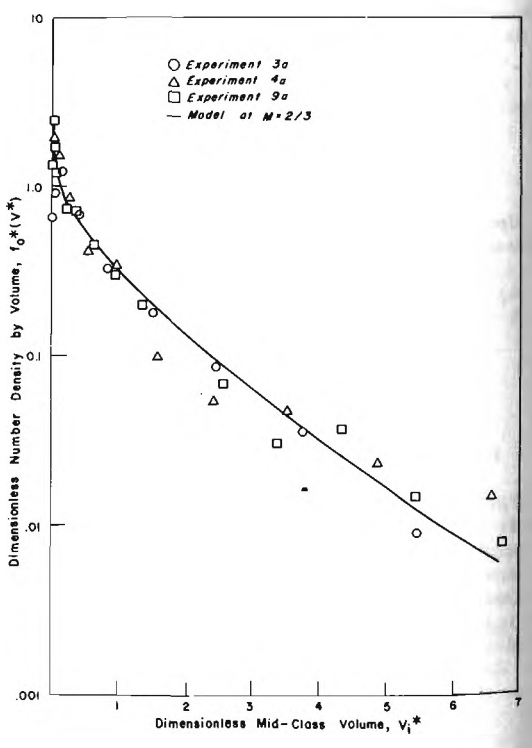

FIGURE 9. Dimensionless drop size distributions with m-values near two-thirds compared to the model at m equal two-thirds.

Values of m for the data obtained in this project ranged from 0.69 to 0.13 with most falling in the neighborhood of m equal to one-half.

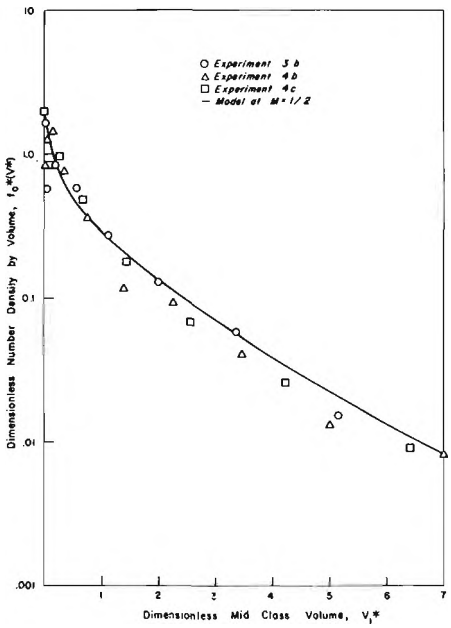

FIGURE 10. Dimensionless drop size distributions with m-values near one-half compared to the model at m equals one-half.

The upper limit of m-values is believed to be in the range of m equal to 0.85 to 1.0 for most conventional solvent extaction systems.

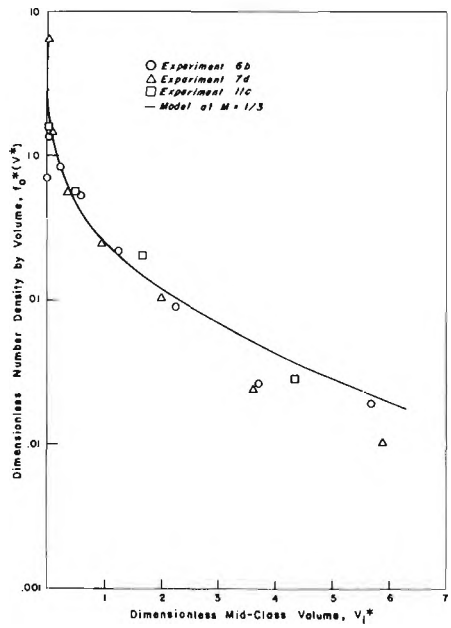

FIGURE 11. Dimensionless drop size distributions for data with m-values near one-third compared to the model prediction at m equal one-third.

Large values of m seem to correspond to low intensity of agitation. Few distributions can be found with m-values larger than one as complete emulsifications of the organic phase cannot occur in these systems. Values of m near zero on the other hand are believed to be the lower limit for the parameter values and these would apply only to very fine, collodial dispersions produced by very intense agitation not commonly used in solvent extaction systems.

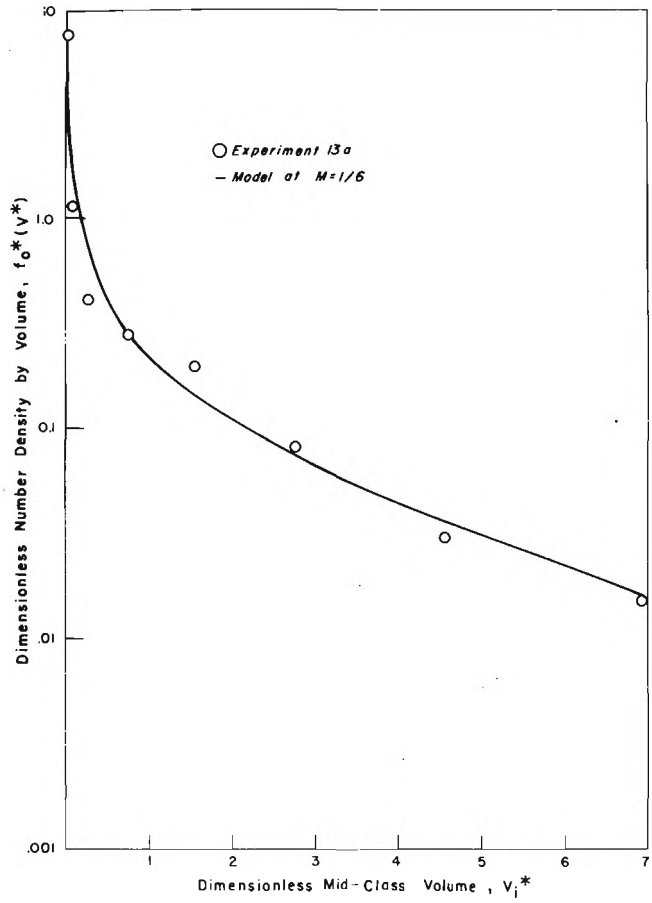

Figure 12. Dimensionless drop size distribution for data with a m-value near one-sixth compared to the model prediction at m equal one-sixth.

It is apparent by now that once the population balance equation has been solved to yield dimensionless size distributions and mean sizes for a reasonable range of m-values, and once equations become availiable for calculating accurate m-values and dimensional mean sizes from the system physical properties and operating conditions, then the entire dimensional size distribution can be predicted.

To demonstrate the validity and accuracy of this procedure the solutions to the population balance equation and Equations 20, 21 and 22 for m and v_o were used to generate the dimensional distributions for several experimental tests conducted during this project as well as experimental tests conducted by other researchers.

Examples of project data versus model predictions are shown in Figures 13 and 14 for cases with m-values ranging from 0.14 to 0.58 (13).

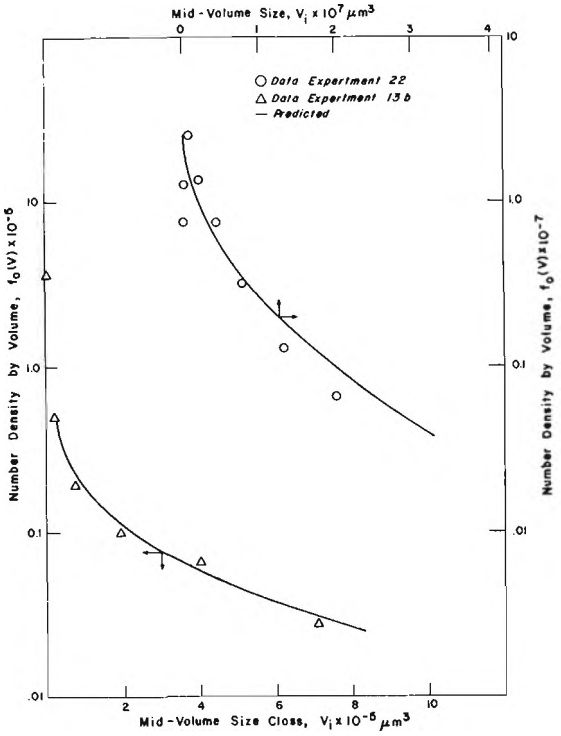

FIGURE 13. Predicted dimensional drop size distributions compared to actual data for experiments 2a and 13b from reference (13).

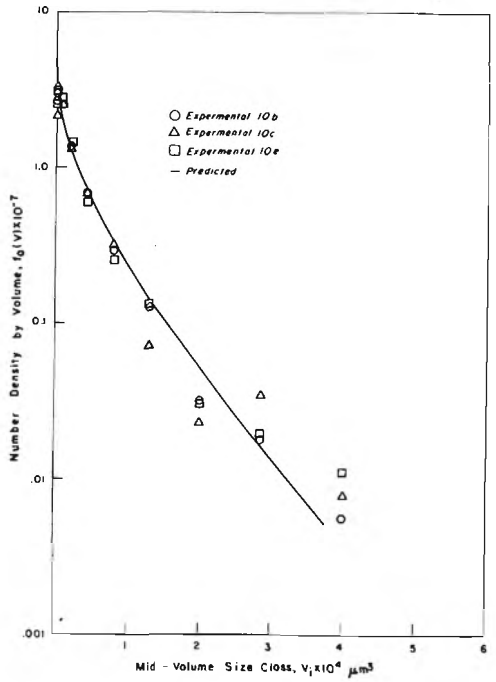

Figure 14. Predicted dimensional drop size distributions compared to actual data for experiments 10b, 10c, and 10e from reference (13).

Examples of data correlations using the results of other researchers are shown in Figures 15 and 16.

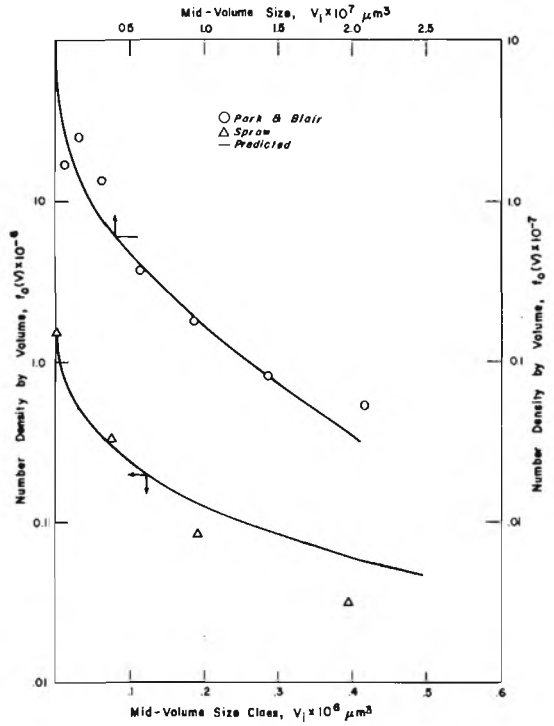

FIGURE 15. Predicted dimensional drop size distributions compared to actual data for the work of Park and Blair (16) and Sprow (22).

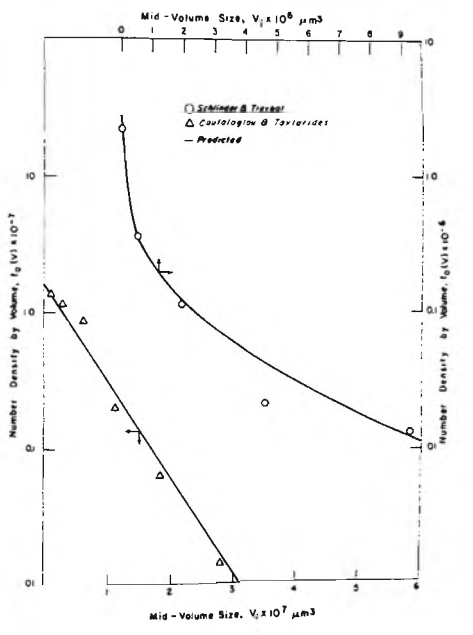

FIGURE 16. Predicted dimensional drop size distribution compared to actual data for the work of Schlinder and Treybal (19) and verification of Equation 19 for the data of Coulaloglou and Tavlarides (6).

The model predictions for the work of Coulaloglou and Tavlarides (5) shown in Figure 16 utilizes the mean size reported by the authors instead of calculating one by Equation 22 since the impeller sizes are quite different.

Summary and Conclusions

Several important variables were found to influence drop size disribution in dispersed phase mixers: (1) agitation time; (2) speed/power input; (3) phase fraction; (4) the presence or absence of an extractant; (5) aqueous pH; and (6) ionic strength of the aqueous. Other factors such as simultaneous chemical reaction and continuous mode operaton at moderate to long retention times seemed to have little effect on size distribution in the system studied.

The model developed here is unique in that it simplifies the mathematics with logical assumptions and reduces the number of adjustable parameters to a minimum via dimensional analysis. This allows one to relate the significant parameters of the model to the system physical properties and operating conditions via simple multiple linear regression expressions. It was demonstrated that this model permits the prediction of dimensional size distributions without experimentation for similar bench scale systems and has considerable potential for future application.

Acknowledgements:

The authors wish to thank The U.S. Bureau of Mines, Salt Lake Metallurgy Center, for partial funding of this research; the Kennecott Copper Corp. for computer time donated to allow numerical solutions of the population balance equations; Mr. Jaime Sepulveda for helpful discussions; and Mr. Jim Smith of the U. of U. Medical Center for assistance in operating the Quanta Met Image Analyzer.

Notation

English

$\overline{B}$	Average change in population due to discrete birth events $((1^{-6}t^{-1}))$
$\overline{B}_b$	Average birth of drops due to breakage events $(1^{-6}t^{-1})$
$\overline{B}_c$	Average birth of drops due to coalescence events $(1^{-6}t^{-1})$
D	Impeller diameter (l)
$\overline{D}$	Average change in population due to discrete death events $(1^{-6}t^{-1})$
$\overline{D}_b$	Average death of drops due to breakage events $(1^{-6}t^{-1})$
$\overline{D}_c$	Average death of drops due to coalescence events $(1^{-6}t^{-1})$
$F_o(d)$	Cumulative number density function by diameter (-)
$f_o(v)$	Number density function for droplet volume (1^{-3})
$f_o^*(v^*)$	Dimensionless number density function by volume (-)
H	Liquid height (l).
k	Selection function constant (variable units)
m	Selection function size dependence parameter
N'_{We}	Modified Weber number (-)
$\overline{n}(t)$	Average number of drops per unit volume (ℓ^{-3})
$\overline{n}^*(t)$	Dimensionless average number of drops per unit volume (-)
Q_{in}	Flow rate into the mixer (1^3t^{-1})
Q_{out}	Flow rate out of the mixer (1^3t^{-1})
S(v,t)	Droplet selection function (t^{-1})
t	Time (t)
t*	Dimensionless time (-)
t_o	Characteristic time-inverse of the coalescence function (t)
V	Total volume of liquid in the mixer
v	Volume of a drop (1^3)
v*	Dimensionless drop volume (-)
$\overline{v}$	Average drop volume (1^3)
v'	Volume of drops in different size classes (1^3)
v_o	Parameter for dimensional analysis (-)
$\overline{v}^*$	Dimensionless mean drop size (-)
v_{max}	Maximum drop volume (1^3)
v_{min}	Minimum drop volume (1^3)
ζ_i	Property of interest.
λ	Coalescence function (t^{-1})
ϕ	Phase fraction (-)
$\overline{\psi}$	Average population density (1^{-6})
$\overline{\psi}^*$	Dimensionless population density (-)
ν_c	Continuous phase kinematic viscosity (1^2t^{-1})
ν_d	Disperse phase kinematic viscosity (1^2t^{-1})
I	Ionic strength $I = 1/2\ \Sigma nC_i(Z_i)^2$.
I_o	Standard ionic strength equal to .75.
$\overline{I}$	Dimensionless ionic strength equal to I/I_o.
x_j	Time rate of change of property ζ_i

References

1. Assenov, A. and Slater, M. J., "Measurement of Drop Size in Liquid/Liquid Systems by Sedimentation," Hydrometallurgy, Vol. 2, Elsevier Scientific Publishing Co., Amsterdam, 1976, p. 157.

2. Bajpai, R. K. and Ramkrishna, D., "A Coalescence Redispersion Model for Drop-Size Distributions in an Agitated Vessel," Chem. Eng. Sci., Vol. 31, 1976, p. 913.

3. Calderbank, P. H., "Physical Rate Processes in Industrial Fermentation," Trans. Inst. Chem. Engs., Vol. 36, 1958, p. 443.

4. Chen, H. T. and Middleman, S., "Drop Size Distribution in Agitated Liquid-Liquid Systems," AIChE Journal, Vol. 13, No. 5, Sept. 1967, p.989.

5. Coulaloglou, C. and Tavlarides, L. L., "Drop Size Distributions and Coalescence Frequencies of Liquid-Liquid Dispersions in Flow Vessels," AIChE Journal, Vol. 22, No. 2, March 1976, p. 289.

6. Coulaloglou, C. and Tavlarides, L. L., "Description of Interaction Processes in Agitated Liquid-Liquid Dispersions," Chem. Eng. Sci., Vol. 32, 1977, p. 1289

7. Fernandes, J. B., and Sharma, M. M., "Effective Interfacial area in Agitated Liquid-Liquid Contactors, " Chem. Eng. Sci., Vol. 22, 1967, p. 1267.

8. Giles, J. W., et.al., "Drop Size Distributions in Agaitated Liquid-Liquid Systems with Simultaneous Interface Mass Transfer and Chemical Reaction," Solvent Extraction Proceedings International Solvent Extraction Conference, Edited by J.A. Gregory, Soc. Chem. Ind., London, 1971, p. 94.

9. Grosssman, G., Determination of Droplet Size Distributions in Liquid-Liquid Dispersions," Ind. Eng. Chem. Process Des. and Develop., Vol. 2, No. 4. 1972, p. 537.

10. Hulburt, H. M. and Katz, S., "Some Problems in Particle Technology. A Statistical Mechanical Formulation," Chem. Eng. Sci., Vol. 19, 1964, p. 574.

11. Komasawa, I., T. Sasakura, and T. Otake, "Behavior of Reacting and Coalescing Dispersed Phase in a Stirred Tank Reactor," J. of Chem. Eng. of Japan, Vol. 2 No. 2, 1969, p. 209.

12. Luhning, R. W., and Sawistowski, H., "Phase Inversion in Stirred Liquid-Liquid Systems," Solvent Extraction Proceedings International Solvent Extraction Conference, Edited by J.A. Gregory, Soc. Chem. Ind., London, 1971, p. 873.

13. Mackelprang, R. B., "Mathematical Modeling of Disperse Phase Mixers," M.S. Thesis, University of Utah, August, 1979.

14. Mlynek, V. and Resnick, W., "Drop Sizes in Agitated Liquid-Liquid Systems," AIChE Journal, Vol. 18, No. 1, Jan. 1972, p. 122.

15. Nishikawa, M., "Drop Size Distribution in a Mixing Vessel," Research Paper, Dept. of Chem. Eng. Kyoto University, Japan, 1975.

16. Park, J. Y. and Blair, L. M., "The Effect of Coalescence on Drop Size Distribution in an Agitated Liquid-Liquid Dispersion," Chem. Eng. Sci., Vol. 30, 1975, p. 1057.

17. Prokop, A., Ludvik, M. and L. E. Erickson, "Growth Models of Cultures with Two Liquid Phases," Biotechnol. Bioeng., Vol. 14, 1972, p. 587.

18. Ritcey, G. M. and Ashbrook, A. W., "Solvent Extraction in Process Metallurgy," Short Course Text sponsored by TMS-AIME, Denver, Colorado, Feb. 1978.

19. Schindler, H. D. and Treybal, R. E., "Continuous-Phase Mass Transfer Coefficients for Liquid Extraction in Agitated Vessels," AIChE Journal, Vol. 14, No. 5, Sept. 1968, p. 790.

20. Shinnar, R., "On the Behavior of Liquid Dispersions in Mixing Vessels," J. Fluid Mech., Vol. 10, 1961, p. 259.

21. Sprow, F. B., "Drop Size Disteributions in Strongly Coalescing Agitated Liquid-Liquid Systems," AIChE Journal Vol. 13, No. 5, Sept. 1967, p. 995.

22. Sprow, F. B., "Distribution of Drop Sizes Produced in Turbulent Liquid-Liquid Dispersion," Chem. Eng. Sci., Vol. 22, 1967, p. 435.

23. Valentas, K. J. and Amundson, N. R., "Influence of Droplet Size-Age Distribution on Rate Processes in Dispersed Phase Systems," Ind. and Eng. Chem. Fund., Vol. 7, No. 1, Feb. 1968, p.66.

24. Vermeulen, T., Williams, G. M., and G. E. Zanglois, "Interfacial Area in Liquid-Liquid and Gas-Liquid Agitation," Chem. Eng. Progr., Vol. 51, No. 2, Feb. 1955, p. 85-F.

25. Herbst, J. A. "Rate Processes in Multiparticle Metallurgical Systems" Chapt. 2 in Rate Processes of Extractive Metallurgy, Ed. H. Y. Sohn and M. E. Wadsworth, Plenum Press, 1979, p. 53.